

# Dust particles in controlled fusion devices: morphology, observations in the plasma and influence on the plasma performance

M. Rubel<sup>a\*</sup>, M. Cecconello<sup>a</sup>, J.A. Malmberg<sup>a</sup>, G. Sergienko<sup>b\*\*</sup>, W. Biel<sup>b</sup>, J.R. Drake<sup>a</sup>, A. Hedqvist<sup>c</sup>, A. Huber<sup>b</sup>, V. Philipps<sup>b</sup>

<sup>a</sup> Alfvén Laboratory, Royal Institute of Technology, Association Euratom–NFR, Stockholm, Sweden

<sup>b</sup> Institute of Plasma Physics, Forschungszentrum Jülich, Association Euratom, Trilateral Euregio Cluster (TEC), Jülich, Germany

<sup>c</sup> Physics Department, Royal Institute of Technology, Association Euratom–NFR, Stockholm, Sweden

**Abstract.** The formation and release of particle agglomerates, i.e. debris and dusty objects, from plasma facing components and the impact of such materials on plasma operation in controlled fusion devices has been studied in the Extrap T2 reversed field pinch and the TEXTOR tokamak. Several plasma diagnostic techniques, camera observations and surface analysis methods were applied for in situ and ex situ investigation. The results are discussed in terms of processes that are decisive for dust transfer: localized power deposition connected with wall locked modes causing emission of carbon granules, brittle destruction of graphite and detachment of thick flaking co-deposited layers. The consequences for large next step devices are also addressed.

## 1. Introduction

The formation of dust particles in magnetic controlled fusion devices with carbon or beryllium/carbon plasma facing components (PFCs) is well established and is one of the consequences of plasma–material interactions [1–9]. The term ‘dust’ refers to small loose particle agglomerates, ranging in size from several tens of nanometres to millimetres, found after long operation periods on the bottom parts of the vessel, in gaps between PFCs and in pumping ducts. Bright objects ‘flying’ in the plasma are also frequently observed during machine operation. These phenomena have recently attracted much interest, and the observations of dust in fusion devices have become more systematic. This is related to its possible influence on plasma stability when particulates enter the confined plasma [10]. The production and re-deposition of dusty objects also reduces the optical transmission of diagnostic windows covered with co-deposits and/or dust particles [11]. There are also serious hazards connected with fuel accumulation (tritium inventory) [3–5, 12–14] and — if grains are formed in substantial

quantities — steam reactions in the case of cooling water leaks into the vessel [7, 12, 15]. Several possible pathways leading to the formation and transfer of dust to the plasma have been discussed: disintegration of thick flaking co-deposited layers [1–8, 16], emission of particles under local high heat flux loads [17] and, as has been tentatively suggested, plasmo-chemical processes occurring in the cool region of the far edge plasma [1]. The reasons and consequences of dust levitation and charging up effects in the plasma have also been thoroughly addressed in very recent times [18].

Detailed investigation of dust in fusion devices is a fairly new field of research and information concerning the behaviour of particles in the plasma and the morphology (composition, structure, magnetic and electric properties, implications for reactor safety, etc.) is somewhat scattered in the literature. On the other hand, such studies lead also to an improved understanding of related phenomena in concepts proposing liquid [19], droplet, fluid or granule (ball) type moving structures for high heat flux components and the first wall. Identification of regions with thick co-deposits and dust or flake accumulation helps to select and develop the most appropriate in situ methods aimed at the prevention of dust formation and the removal of fuel containing material [20].

\* Corresponding author.

\*\* *Permanent affiliation:* Association IVTSN, Institute of High Temperatures of the Russian Academy of Sciences, Moscow, Russian Federation.

This work is focused on the examination and comparison of dust particles produced under various plasma operation conditions in a reversed field pinch (RFP) and in a tokamak. Herewith, we make an attempt to bring together and interpret a number of in situ and ex situ observations regarding solid agglomerates penetrating into the plasma and influencing its performance. The main interest and emphasis is on the discrimination between the various mechanisms underlying dust formation, on the morphology of grains and on their behaviour in the plasma.

## 2. Experimental set-up

We report on the studies carried out in the Extrap T2 RFP [21–23] and in the TEXTOR tokamak [24]. These are two different types of toroidally axisymmetric device when the timescale and modes of operation are considered. However, features common to the two machines are related to the graphite PFC and also to high particle fluxes (of the order of  $1 \times 10^{23} \text{ m}^{-2} \text{ s}^{-1}$ ) to the wall which are decisive for material erosion and transport, both local and global. In this sense, studies of erosion–deposition and the dust formation mechanism are representative and allow conclusions on processes in large scale machines, such as JET, also strongly addressing the issue of flake formation in remote areas [14]. Last but not least, the operation of Extrap T2 and TEXTOR with non-radioactive hydrogen isotopes (D, H) enables personnel entry to the vessel and the direct investigation of wall erosion and the collection of dusty objects.

Extrap T2 is a medium sized RFP at the Alfvén Laboratory, Stockholm, operated for several years (1994–1998) with the former (Ohmically Heated Toroidal Experiment (OHTE) [25]) vessel and a complete graphite liner consisting of several thousand small tiles:  $2.5 \text{ cm} \times 3.2 \text{ cm}$  and  $2.5 \text{ cm} \times 12.5 \text{ cm}$ . Figure 1 shows a part of the inner Extrap T2 wall. TEXTOR is a medium sized tokamak operated at the Forschungszentrum Jülich and its mission is focused on plasma–surface interactions [24]. Inside the vacuum vessel there is an Inconel liner, heated to a temperature of up to  $350^\circ\text{C}$ , and arrays of graphite PFC poloidal limiters and ICRF antenna protection tiles (both types are positioned in the SOL), an inner bumper limiter and a toroidal belt pump limiter (Advanced Limiter Test (ALT-II) [26]). The latter, consisting of eight blades each covered with 28 tiles, is the major PFC of TEXTOR. The total



**Figure 1.** View of the inner wall of the Extrap T2 vacuum vessel after thousands of plasma discharges, with full coverage provided by small graphite tiles. Some imperfections in the alignment of the tiles and damage to the tile edges are visible.

surface area of ALT is  $3.4 \text{ m}^2$ , corresponding to about 9% of the inner wall area.

CCD cameras were used for the observation of dusty objects in the plasma. At Extrap T2 a Pulnix camera with an IR filter ( $1040 \pm 20 \text{ nm}$ ) was installed either on a bottom port (toroidal angle  $330^\circ$ ) or on a tangential port. Dependent on the location, the field of view was limited to 3 and 11% of the vessel volume, or 1 and 5% of the wall area, respectively. The temperature of recorded objects could be estimated in the range between  $850^\circ\text{C}$  (noise level) and  $1200^\circ\text{C}$  (signal saturation). The cameras used at TEXTOR viewed in the toroidal direction searching approximately 25% of the vessel volume. A Sony CCD recorded in the visible range (400–700 nm), whereas a Hitachi device was recording in the visible to a near IR range (400–1000 nm), therefore, producing images mostly in  $\text{D}_\alpha$  and C II light. In all cases, the image integration time was 20 ms, which — in the case of Extrap — was longer than the pulse duration, typically 7–12 ms.

Following operational periods comprising several thousand plasma discharges (corresponding to about 50 s at Extrap T2 and 17 290 s at TEXTOR), the machines were opened and dust particles collected from the PFCs and the diagnostic windows. A vacuum cleaner with a specially designed filtration system was used. On the suction duct of the cyclone vacuum cleaner a container (10 cm in diameter) was mounted, acting as a dust collector, lined with a layer of filtration paper supported by a fine metal mesh.

The dust was sucked to the collector through soft tubing made of medical grade silicon rubber. Using this procedure scraping (and the resulting disintegration) of co-deposits was avoided, because the aim was to collect only loose particulates present on the vessel bottom and in gaps between the graphite tiles of the PFCs. At Extrap T2, the collection was accomplished through the ports (maximum flange diameter 63 mm) and the dust was collected from about 30% of the inner wall area. At TEXTOR, the collection was performed during personnel entry to the vessel and, therefore, the dust was sucked from the complete bottom of the liner and limiter tiles. Another set of dust samples was gathered from the rear side of the ALT-II supporting wing (stainless steel), graphite scoops, particle neutralizers and pumping duct. The dust and thick co-deposits were swept from the above mentioned substrates. This was done when one of the eight limiter blades was dismantled after serving for three years in the machine, then corresponding to about 90 000 s of plasma operation.

The dust was investigated by means of scanning electron microscopy (SEM), nuclear reaction analysis (NRA), thermal desorption spectroscopy and energy dispersive X ray spectroscopy (EDS) using a windowless silicon LINK detector of Oxford Instruments.

### 3. Results and discussion

#### 3.1. Observations in the plasma

##### 3.1.1. Extrap T2

In the IR image shown in Fig. 2 tracks of glowing dusty objects passing through the plasma during a discharge are shown. Track orientation with respect to the toroidal direction, path lengths and radial position with respect to the reversal surface (RS) can be inferred for the tracks labelled (a), (b) and (c). The results are collected in Table 1. The calculation of track length and radial position is based on two assumptions. The first one is that dust particles are forced to move along magnetic field lines. This can be explained by a rocket-like phenomenon caused by the electron heating which induced the emission of particles. The second assumption is that the plasma is in a fully relaxed state where the magnetic field profiles are described by the Bessel function model (BFM) [27]. From this model, the angle  $\alpha$  between the magnetic field and the toroidal direction is calculated as a function of the radial co-ordinate. Comparison between the observed angles formed by tracks

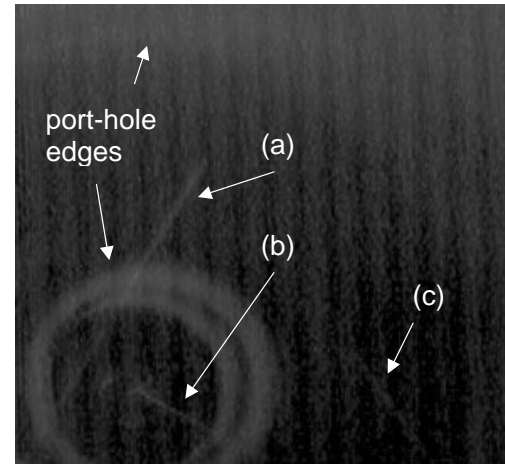


**Figure 2.** IR image recorded during a discharge at Extrap T2. The tracks of dust particles ((a)–(c)) are indicated.

**Table 1.** Characteristics of dust tracks in the EXTRAP T2 plasma

Track	Path length (mm)	Angle (deg)	Radial position (cm)
(a)	23	20	17.4 (outside RS)
(b)	11	30	6.2 (inside RS)
(c)	13	60	8.8 (inside RS)

(a), (b) and (c) with respect to the toroidal direction and  $\alpha(r)$  gives their radial positions. Eventually, from simple geometric considerations, the track length is calculated. Unfortunately, the analysis of the thermal image itself does not allow the determination of particle size and the exact position of the origin. The frame integration time (20 ms) also makes it difficult to conclude at which moment during the discharge the particles appeared.

Figure 3 shows a reconstruction of the LCFS based on the  $m = 1$  magnetic signal measured by pick-up coils which reflect fluctuations of the radial magnetic field. The magnetic diagnostic of Extrap T2 consisted of an array of pick-up coils (6 poloidal  $\times$  32 toroidal positions). This is described in detail by Hedin [22], whereas the procedure of the LCFS reconstruction is given in Ref. [28]. The plot clearly proves that the wall locked mode occurred at a toroidal angle of  $330^\circ$ , i.e. exactly in the position viewed by the camera. The evolution of the magnetic signal plotted versus the discharge time, shown

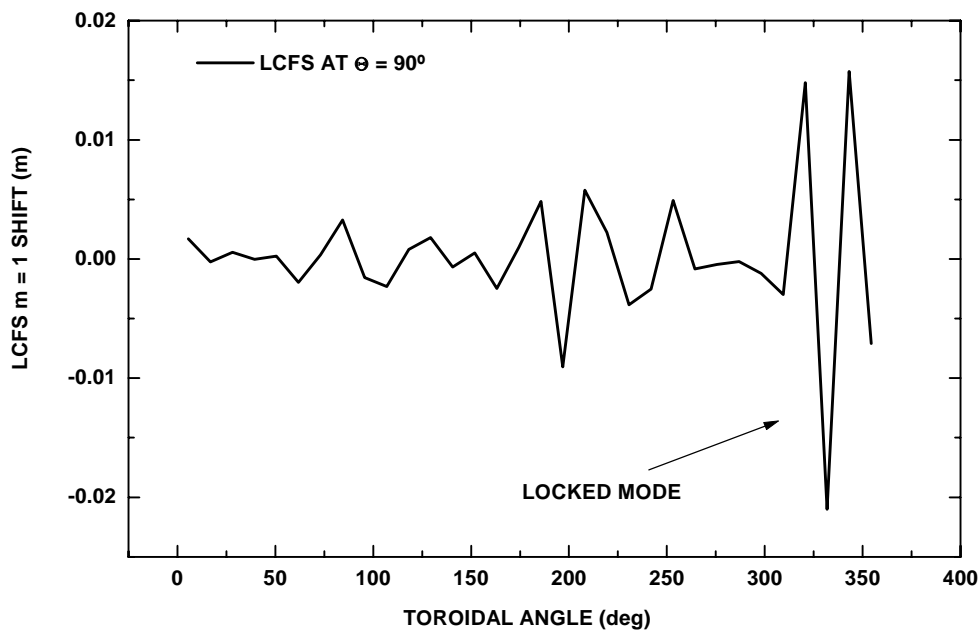


**Figure 3.** Magnetic signal plotted versus toroidal position of the pick-up coils during a discharge where dust particles were detected.

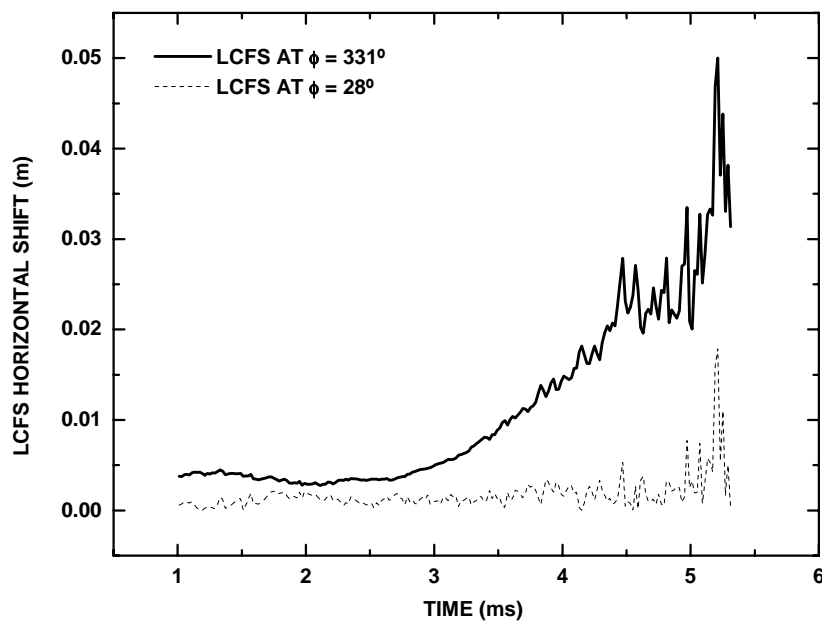


**Figure 4.** Magnetic signal plotted versus the discharge time at Extrap T2; the signal was recorded during a discharge when dust particles were detected at the position of the locked mode (toroidal angle  $331^\circ$ ) and at a position located far from the locked mode (toroidal angle  $28^\circ$ ).

in Fig. 4, indicates a locked mode growing steadily to the end of the discharge which is then terminated abruptly at 5.5 ms. A correlation between the locked

mode and the presence of dust makes it fairly plausible that small graphite debris were ejected due to local energy deposition by wall locking of the plasma.

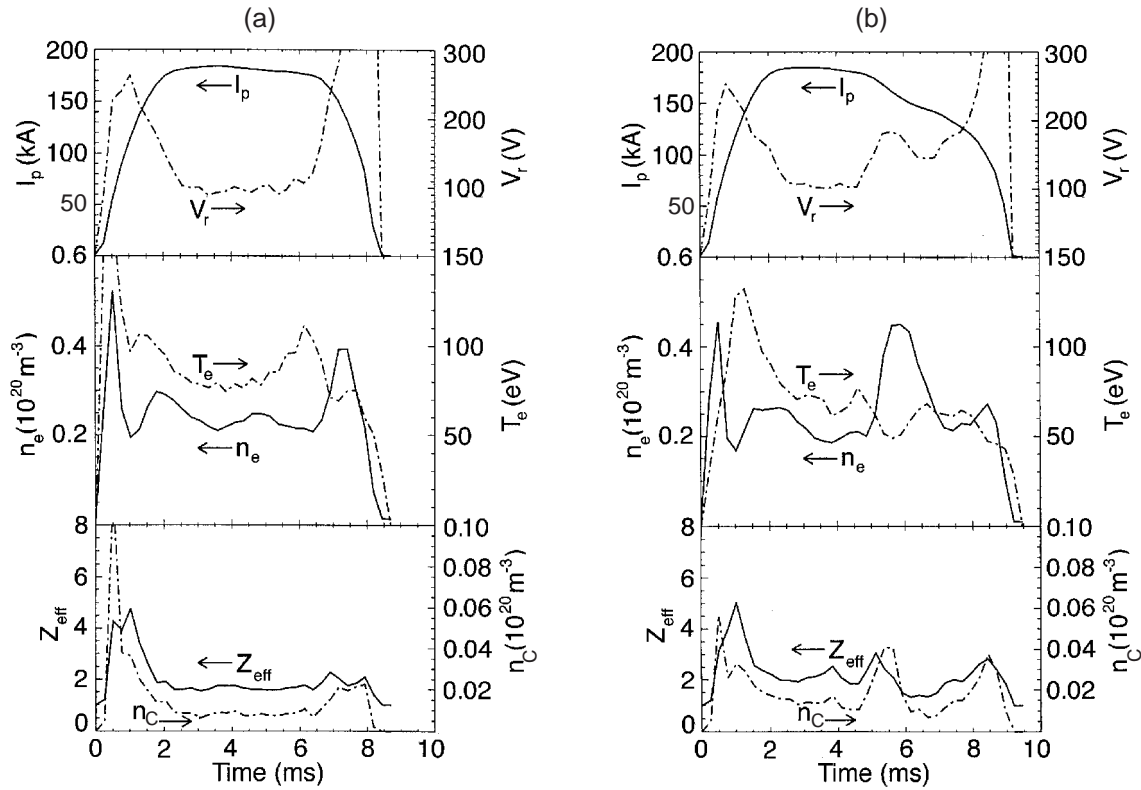


**Figure 5.** Signals recorded during discharges at Extrap T2. Traces of plasma current  $I_p$ , loop voltage  $V_r$ , line averaged density  $n_e$ , electron temperature  $T_e$ , effective charge  $Z_{eff}$  and carbon density  $n_C$  plotted versus the discharge time: (a) a discharge without significant impurity influx and (b) a discharge with a significant influx of carbon impurity.

It causes not only intense chemical erosion but also the ejection of small graphite clusters [17, 29] and even so-called brittle destruction of the PFC [30]. Brittle destruction is a threshold type phenomenon observed for graphite (for instance EK98) at power loads exceeding  $360 \text{ MW m}^{-2}$ . The area loaded during a wall locked mode varies from discharge to discharge, but it can be estimated as between 20 and  $500 \text{ cm}^2$ . Taking into account the energy stored in the plasma (2000 J) and the timescale of wall locking (1 ms), the power locally deposited during the process ranges from  $40 \text{ MW m}^{-2}$  to at least  $1000 \text{ MW m}^{-2}$ . Therefore, in some events, the threshold for brittle destruction and ejection of particles is overcome. This is in agreement with the fact that dust is detected only in some discharges. On the basis of a visual inspection of damaged in-vessel components it may also be suggested that the field on interaction is much smaller and the release of larger debris (i.e. in submillimetre size) occurs predominantly on the edges of non-perfectly aligned graphite tiles, see Fig. 1. Thus, one can tentatively conclude

that the mechanism of dust ejection at Extrap T2 is, to some extent, analogous to that observed under electron beam irradiation of graphite [17, 30].

The correlation of dust injection into the plasma with local magnetic measurements also contributes to a better understanding of the evolution of the fundamental signals ( $n_e$ ,  $T_e$ ,  $I_p$ ,  $Z_{eff}$ ,  $V_r$ ) and carbon density  $n_C$ . The latter values were calculated taking into account the sum of the intensities of the CIV and CV lines. Other ionization states of carbon were neglected as their contribution to the density was orders of magnitude smaller. Although all discharges at Extrap T2 are wall locked, two clear types of temporal evolution of those signals have been observed [31]:

- (a) Fairly smooth profiles during the flat-top phase;
- (b) Profiles indicating a sudden impurity (carbon) influx at a certain moment during the pulse.

This is illustrated by the traces plotted in Figs 5(a) and (b) for discharges without and with significant influxes of impurity atoms, respectively. Under

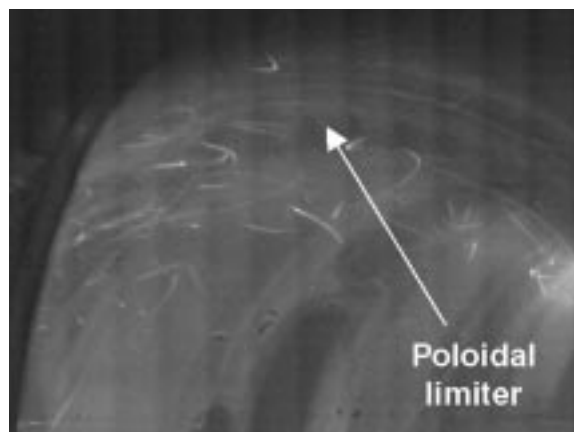


**Figure 6.** Example of dust particles released from the main upper poloidal limiter (indicated by the arrow) during the startup phase of a discharge at TEXTOR.

normal operational conditions, as shown in Fig. 5(a), the major mechanism for carbon influx to the plasma is chemical erosion of graphite PFC [32]. However, in the case presented in Fig. 5(b), the sudden increase in the carbon content followed by a distinct density fluctuation is most probably attributed to the appearance of graphite debris penetrating the plasma.

### 3.1.2. TEXTOR

Flying dusty objects at TEXTOR have also frequently been observed. It is known that after prolonged operational periods, the limiters and protection tiles of ICRF antennas are covered with a co-deposited layer containing mainly carbon and hydrogen isotopes but also significant amounts of other species (e.g., B, Si, Ni, Cr, Fe) [3, 33, 34]. These layers, even some hundreds of microns in thickness, are of either columnar [2, 3, 33] or stratified [35] structure. They are very brittle and disintegrate easily, peeling off from the graphite substrate. In some spots, there are 10–15  $\mu\text{m}$  broad gaps in the deposit to substrate boundary [16, 33]. Thermal conductivity of co-deposits differs from that of graphite and the surface temperature rise strongly depends on the thermal contact between the co-deposit and the substrate. The co-deposit adherence varies from one location to another, and loosely bound flakes produce ‘hot spots’, which can easily be seen in large area CCD images. Because of poor thermal contact and adherence, the layers peel off under thermal loads and also due to arcing. Some of the flakes contain small metal droplets formed by erosion of metal surfaces, far in the SOL, during off-normal events (probably runaway electron production). The

droplets condensed at other places, forming charged islands under the influence of the magnetic field.

A release of particles or even a production of particle clouds originating from the main poloidal limiter is shown in Fig. 6. The granule trajectories are not straight, but follow closely the magnetic field lines. This indicates that the objects are electrically charged by the incoming fast electron flux. As the camera records in the visible range and the TEXTOR co-deposits are known to contain 5–16% deuterium [3, 16], the light emitted is mostly associated with  $\text{D}_\alpha$  and the continuous radiation stimulated by ablation of the material. Observations, such as those documented in Fig. 6, are mainly made at the beginning of discharges. This might be associated with arcing which predominantly occurs during the startup phase. One may speculate about the magnetic field acting on the debris due to the rising poloidal magnetic field. In the cases under consideration, the dust production did not prevent the pulse developing. No significant influence on the fundamental signals was observed but, on some occasions, an increase of the carbon signal was recorded. The problem of the dust appearance at the beginning of the discharge may partly be tackled by machine conditioning using ICRF pulses [36] in combination with RF assisted startup, i.e. pre-ionization before the ohmic power

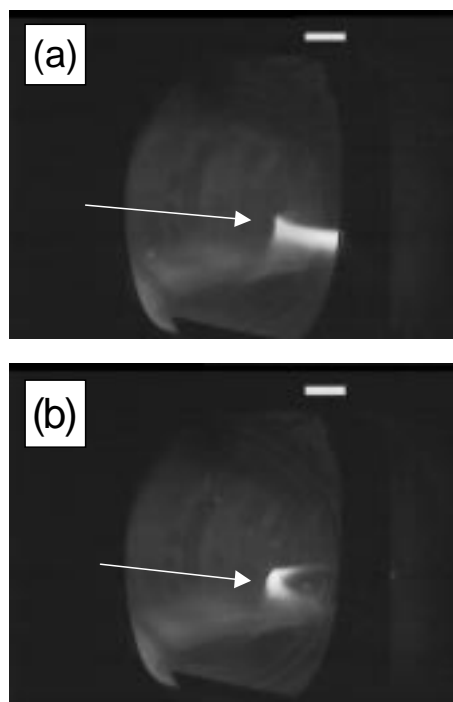


**Figure 7.** An example of a debris motion caused by the rocket effect. Moving debris on the high field side of the torus is indicated by the arrows.

has been applied. The method has been tested at TEXTOR [37] and Tore Supra [38]. This procedure improves the reliability of initial breakdown but it prevents formation of co-deposits and does not influence their growth rate.

Dust release events are, however, neither time nor place specific, i.e. they occur not only in the initial phase or on the poloidal limiters only. Figure 7 shows debris (the bright trace) travelling during a developed discharge on the high field side of the torus. From this we conclude that debris originates from the inner bumper limiter. The rocket-like effect in the particle motion is related to the difference in heat fluxes from the ion and electron drift sides. As a consequence, unbalanced forces stimulate the debris motion because of stronger heating from one side.

The images in Figs 8(a)–(d) show a time sequence illustrating the release and behaviour of solid particles in the torus. They have been recorded on eight consecutive frames (i.e. during 160 ms) in the upper part of the high field side. For the presentation we have selected four representative CCD images. This may indicate that they originate from the upper tiles of the inner bumper limiter. The process is depicted during the auxiliary plasma heating by neutral beams of a discharge performed shortly after the machine opening (venting) followed by a fresh boronization. One may suggest that the dust release was stimulated both by the increased heat flux to the wall and the accompanying slight shift in the plasma position. Simultaneous spectroscopic measurements allow the identification of the

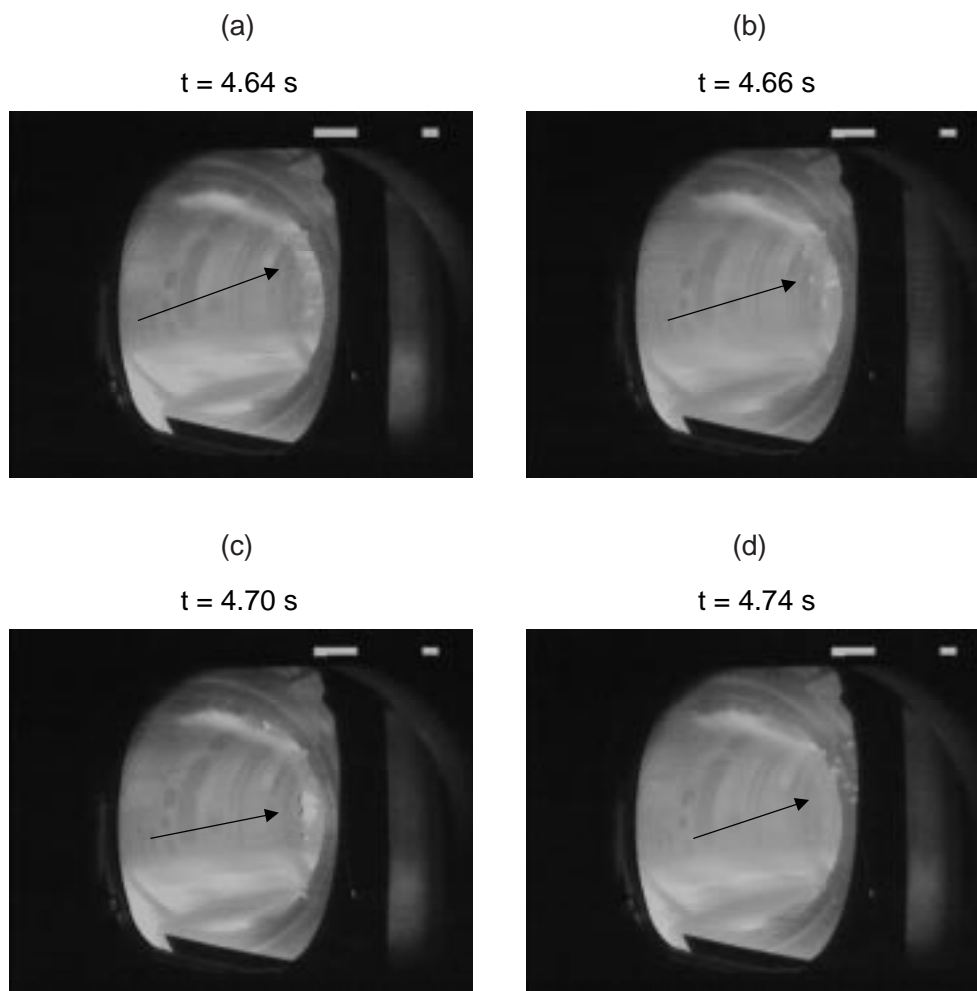


**Figure 8.** A time sequence showing a cloud of particles released during a discharge at TEXTOR. The cloud visible on the upper part of the high field side is indicated by the arrows.

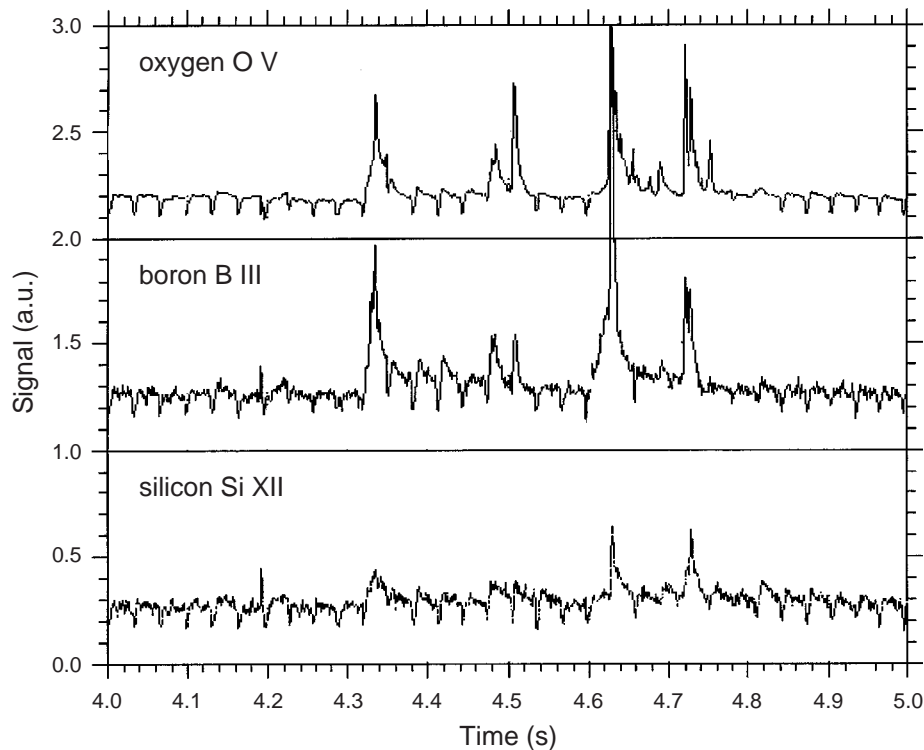


**Figure 9.** Spectroscopic signals recorded during the dust release shown in Fig. 8.

composition of ablated species: oxygen, boron and silicon originating from earlier siliconization. This is documented by the plots in Fig. 9. The fluctuations of the O V, B III and Si XII traces, in the time interval between 4.60 and 4.74 s, perfectly coincide with the appearance of dust in the camera field of view. From the same plots one can conclude that another event of dust release and ablation occurred earlier (4.32–4.52 s) in the part of the torus that is not viewed by the camera. During the time interval under discussion, there is — as expected — a certain density increase and enhanced fluctuations in the level of power radiated. These changes are relatively small and, from this, one can conclude that the dusty cloud consisted of fairly small objects. The high luminosity of the ablated material makes a direct size determination impossible. However, the upper limit of the particles' thickness can be estimated to be less than  $0.5\ \mu\text{m}$ . This estimate is based on the fact that the dust does not contain much carbon (no fluctuation of the C signal is observed) and, therefore, it is reasonable to suppose that the objects are mostly flakes of the boronized layer whose usual thickness is several hundred nanometres. All the above conclusions are in agreement with results found by Nahihara et al. [10], who did not observe the influence of small carbon

agglomerates (less than  $2\ \mu\text{m}$  in diameter) dropped into the JIIP-T-IIU vessel during a discharge. In addition, recent experiments [39] have shown that developed discharges did not disrupt when carbon pellets of a millimetre size were injected into the plasma.

Knowledge of the surface morphology of the limiters, together with the results presented above, indicates that the objects recorded as dust particles are predominantly loosely bound flakes of co-deposited layers which become detached from the major PFC due to high power loads and, possibly, electric forces. This statement does not exclude other pathways for dust formation at TEXTOR, such as ejection of graphite agglomerates and brittle destruction caused by runaway electron production. The size of the fraction of graphite debris collected from the vessel and also the damage to some PFCs may indicate that brittle destruction takes place on certain occasions.

### 3.2. Morphology

#### 3.2.1. Extrap T2

The amount of material collected with a vacuum cleaner from approximately 30% of the inner vessel wall was in the milligram range, i.e. below 1 g. The majority of dust particles was in the size range from



50 to 250  $\mu\text{m}$  but, in general, two classes could be distinguished, such as graphite debris with sharp edges of about 1 mm in length and much smaller objects. These smaller grains belonged, in turn, to four categories identified as follows:

- (a) Tiny agglomerates of submicron size (50–120 nm, these accounted for less than 1% of the mass collected) which can be studied only with a transmission electron microscope [40];
- (b) Very thin fibre-built flakes about 1 mm in thickness but up to about 50  $\mu\text{m}$  in length and width, which accounted for about 5% of the mass collected;
- (c) Grains with sharp edges: graphite debris and disintegrated co-deposits peeled off from the wall (the majority were below 300  $\mu\text{m}$  in size, with a few larger debris of millimetre size). They accounted for approximately 70% of the mass collected.
- (d) Objects with fairly smooth rounded edges and even grains of regular spherical or oval shape, of 20–200  $\mu\text{m}$  in diameter.

In the latter case, the quasi-spherical shape might be attributed to the surface ‘smoothing’ stimulated by the material ablation that occurred when debris passed through the plasma during discharges of a few milliseconds. The possibility that some grains were recycled cannot be excluded, i.e. that they were moved from the floor and transported in the plasma several times during consecutive discharges. The SEM images in Figs 10(a)–(c) exemplify some of the identified structures. The images show: (a) a spherical particle and the thin flakes of co-deposits, (b) a piece of debris with rounded edges and (c) a large piece of debris partly covered with flakes and spherical particulates. The main constituents were carbon and hydrogen with some traces of boron, a result of the earlier solid target boronization of the device wall [41].

### 3.2.2. TEXTOR

Various structures, although not so regular in shape as those described above, are also found when studying the material collected at TEXTOR. Examples are shown in Figs 11(a)–(c). The appearance of dust and flakes resembles, to a great extent, the structure of the co-deposited layer [3, 16]. Their typical thickness is in the range from 40 to 150  $\mu\text{m}$ , while the size of flakes reaches several millimetres. The flakes are brittle (being easily disintegrated into

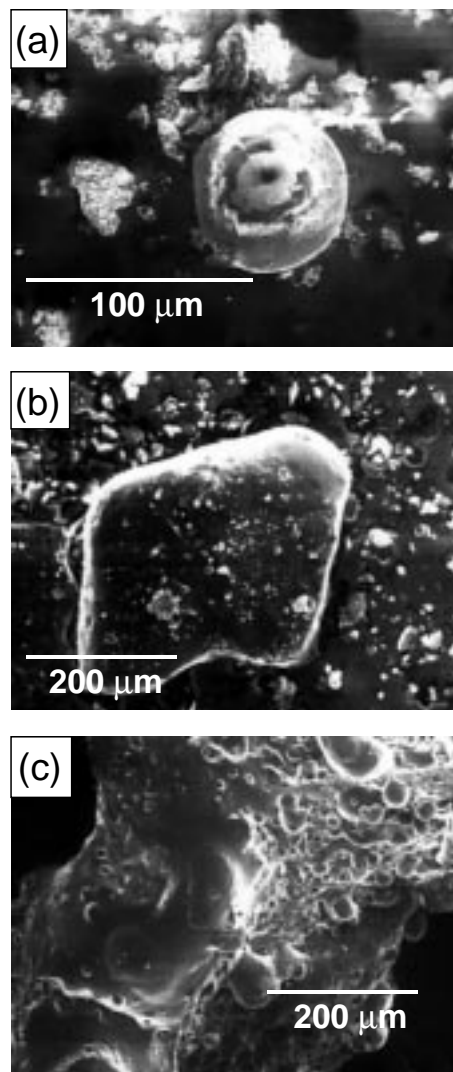


**Figure 10.** Structure of dust collected from the Extrap T2 vessel: (a) a spherical grain and thin co-deposits, (b) a grain with rounded edges, (c) a large piece of debris with co-deposits and spherical particulates.

smaller fragments, as shown in Fig. 11(b)) and, therefore, the exact size distribution cannot be determined. One concludes that these are mostly debris of brittle and flaking co-deposits peeled off from the limiters. As proven with several analytical methods, the dust is mainly composed of carbon and deuterium (5–16 at.%). The presence of other elements is associated with wall conditioning (B from boronization [42], Si after siliconization [43]) and erosion of an Inconel liner (Ni, Cr, Fe, Mo as sputtered atoms and metal droplets) and high  $Z$  limiters (W) tested as candidate PFCs [44–47].

Another question is the estimation of the total dust content in the machine after a long

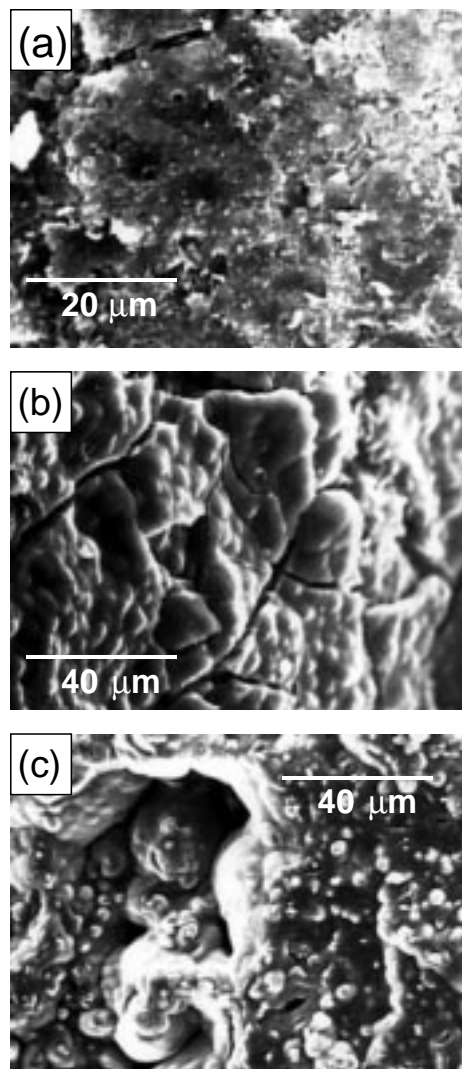


**Figure 11.** Various structures of dust collected from the TEXTOR vessel after 17 290 s of plasma operation. Image (b) shows a broken flake.

operation period. The issue is related to the assessment of the fuel inventory (especially the tritium inventory in DT operated devices) in loose material such as dust grains. The weight of material collected by direct vacuum cleaning of the TEXTOR floor and other wall components after 17 290 s of plasma operation amounted to about 1 g. This result agrees with that reported by Peacock et al. [4], who also collected little material by direct vacuuming of the JET vessel, whereas much greater amounts of loosely adhered material were gathered by smearing of co-deposits, especially in the remote areas in the divertor region. This was also the case in TEXTOR, where significant quantities of co-deposits were found in remote areas such as pumping ducts and other

structures of ALT-II, which were inspected after about 90 000 s of plasma operation. Particle neutralizers, scoops and the rear side of the metal blades supporting the graphite tiles of this limiter were covered by brittle co-deposits with a thickness of up to 1 mm. The scoop covered with the co-deposit is shown in Fig. 12(a), whereas the SEM micrograph in Fig. 12(b) illustrates its structure. This subject will be studied in detail when TEXTOR is closed for a few months in order to accomplish the installation of a dynamic ergodic divertor. Our present estimates, based on the amount of dust and thick co-deposits (several grams) collected from one of the eight limiter units, predict the total dust content in the machine to be over a hundred grams.

#### 4. Summary and conclusions

We have tried to combine in situ and ex situ observations of dust particles in fusion devices in order to better understand the formation mechanism and to infer the impact of dust on plasma behaviour. The correlation has been found, but we want to stress severe technical difficulties accompanying the observation and characterization of the dust release processes. These are highly localized phenomena. Therefore, success in the search for coincidence between the appearance of dust in the plasma and the response in the fundamental and spectroscopy signals is highly limited by the camera's field of view. In neither case under investigation did a release of dust directly lead to major transient events, such as a disruption. However, this result has only been obtained for the observed debris of small size entering the plasma. Recent experiments with controlled injection of carbon pellets (0.5 mm in diameter and 2 mm in length) have not led to a major disruption [39], but larger objects would cause major transient effects.

Comparison of dust particles in the two devices indicates that the species are born in two different processes with respect to the energy and timescale of events. In RFP, the main pathway for dust formation and release is related to high power deposition by wall locked modes resulting in the ejection of small carbon agglomerates and, in some cases, in brittle destruction of the graphite PFC. In tokamaks, dust particles appear in the plasma mostly as a consequence of detachment of flaking co-deposited layers. These are the prevailing pathways in the two devices. Thus, studies performed on two types of carbon wall machine have allowed discrimination of two erosion processes underlying the dust

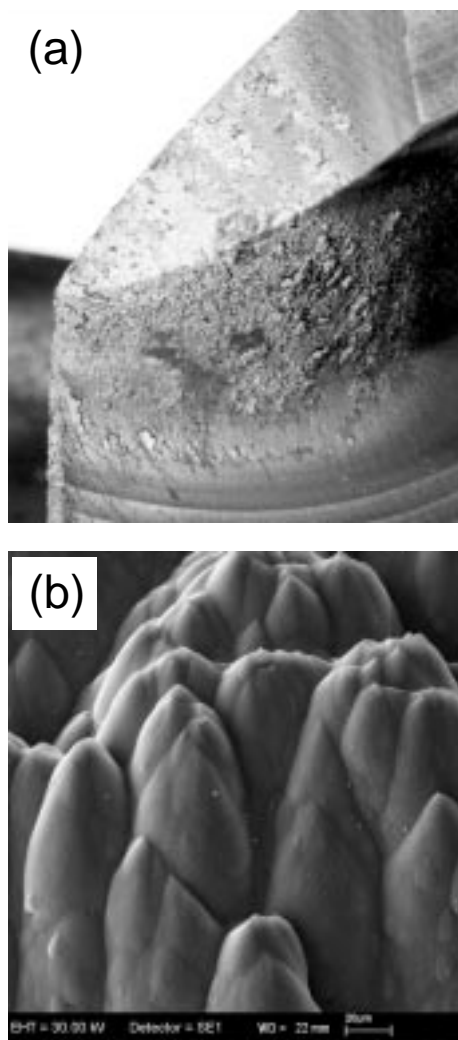


**Figure 12.** Thick co-deposits (up to 1 mm) found after 90 000 s of plasma operation on the rear side of the toroidal belt pump limiter at TEXTOR: (a) a graphite scoop covered with the brittle co-deposited layer; (b) an example of the co-deposited structure.

production. However, for a given device, one mechanism does not exclude the another. To a certain extent, the formation and detachment (peeling off) of co-deposits may play a role in RFP: increased hydrogen and carbon fluxes to the wall during the mode locking phase result in enhanced material transport and, as a consequence, in the high growth rate of co-deposits. A growth rate of the order of a hundred  $\text{nm s}^{-1}$  was observed at Extrap [40], but the total thickness of the layer was relatively small because of the short (50 s) total plasma operation period. On the other hand, in tokamaks, the impact of brittle destruction on PFC erosion (i.e. production of graphite grains) caused by wall locked modes,

vertical displacement events (VDEs) or giant ELMs is predicted [30, 48, 49]. Wall locking, for instance, is a known precursor of disruptions in large machines (such as JET). However, the majority of dust collected in tokamaks after long operation periods is the amorphous material originating from the disintegration of flakes. Therefore, detecting small crystalline graphite grains and separating them from amorphous matter creates severe technical difficulties.

Looking at the consequences of these phenomena in a broader perspective, it remains clear that — independently of the machine (type and size) and the mechanism prevailing — dust formation will always be associated with carbon walls. The same effects of dust and flake formation in shadowed, remote and cooler parts of the machines have been reported from large devices (e.g. louvers in the JET divertor [14]) and from smaller devices [40]. The amount accumulated is perceived to increase with the operation time. Therefore, in ITER-like devices, the accumulation of vast quantities of dust and/or flaking co-deposits [49] is expected, but this must be avoided for various aspects of reactor safety (refer to the Introduction). All these issues are understood to be of crucial importance when the selection of materials for PFCs in next step large devices (such as ITER) with burning plasma is being considered. There are two ways of dealing with the problem: either to eliminate carbon and replace it by metal PFC (e.g. beryllium or high  $Z$  metals) or to develop reliable methods for the removal of dust and co-deposits. Material selection has always been a trade-off issue and, as such, it has been perceived as one of the most difficult problems in fusion engineering. Graphite and its fibre composites have excellent thermomechanical properties and, for that reason, these materials cannot easily be eliminated from the list of candidates for the first wall. Therefore, several novel concepts for reducing the tritium inventory, removing co-deposits and avoiding significant accumulation of dust have recently been proposed and thoroughly reviewed [20]: photocleaning and liquid wash and flush methods. Their further development and application remain to be seen, because there are severe technical difficulties associated with the implementation of these methods in a reactor. Experimental studies carried out in large and small devices allow the identification and prediction of regions with significant co-deposit formation and dust accumulation. This may certainly help the development of location specific in situ methods for the determination of co-deposit growth and dust removal by optical or mechanical means.

## Acknowledgements

The authors are grateful to J. Linke from the Forschungszentrum Jülich and to J. Winter from the Ruhr University, Bochum for discussions. The Extrap team thanks M. Valisa and R. Pasqualotto of the RFX Consorzio (Padua) for supplying the Pulnix camera and R. Pugno for his assistance. A. Vevecka-Priftaj is acknowledged for assistance in SEM studies. We gratefully acknowledge the Wallenberg Foundation for funding the SEM and EDS equipment. The work was partly supported by NFR Contracts Nos F-AA/AU 06571-317 and F-FF 6571-321.

## References

- [1] Winter, J., Plasma Phys. Control. Fusion **40** (1998) 1201.
- [2] Winter, J., Gebauer, G., J. Nucl. Mater. **266–269** (1999) 228.
- [3] Rubel, M., von Seggern, J., Karduck, P., Philipps, V., Vevecka-Priftaj, A., J. Nucl. Mater. **266–269** (1999) 1185.
- [4] Peacock, A.T., et al., J. Nucl. Mater. **266–269** (1999) 423.
- [5] Carmack, W.J., Smolik, G.R., Anderl, R.A., Pawelko, R.J., Hembree, P.B., Fusion Technol. **34** (1998) 604.
- [6] Carmack, W.J., McCarthy, K.A., Petti, D.A., Kellman, A.G., Wong, C.P.C., Fusion Eng. Des. **39&40** (1998) 477.
- [7] Anderl, R.A., et al., J. Nucl. Mater. **258–263** (1998) 750.
- [8] Chappuis, P., et al., J. Nucl. Mater. **290–293** (2001) 245.
- [9] Winter, J., Dust — A New Challenge in Nuclear Fusion Devices? (in preparation).
- [10] Nahihara, I., et al., Nucl. Fusion **37** (1997) 1177.
- [11] Voitsenya, A., et al., J. Plasma Fusion Res. SERIES **3** (2000) 270.
- [12] McCarthy, K.A., Petti, D.A., Carmack, W.J., Smolik, G.R., Fusion Eng. Des. **42** (1998) 45.
- [13] Federici, G., et al., J. Nucl. Mater. **266–269** (1999) 14.
- [14] Coad, J.P., et al., J. Nucl. Mater. **290–293** (2001) 224.
- [15] Piet, S.J., et al., in Fusion Engineering (Proc. 17th Symp. San Diego, 1997), Vol. 1, IEEE, Piscataway, NJ (1998) 167.
- [16] Rubel, M., Vevecka-Priftaj, A., Philipps, V., Mater. Sci. Eng. A **272** (1999) 174.
- [17] Bolt, H., Linke, J., Penkalla, H.J., Terret, E., Phys. Scr. T **81** (1999) 94.
- [18] Winter, J., Fortov, V.E., Nefedov, A.P., J. Nucl. Mater. **290–293** (2001) 509.
- [19] Abdoe, M.A., APEX Team, Fusion Eng. Des. **45** (1999) 145.
- [20] Counsell, G.F., Wu, Chung Hsiu, Phys. Scr. T **91** (2001) 70.
- [21] Drake, J.R., et al., in Fusion Energy 1996 (Proc. 16th IAEA Int. Conf. Montreal, 1996), Vol. 2, IAEA, Vienna (1996) 193.
- [22] Hedin, G., Plasma Phys. Control. Fusion **40** (1998) 1529.
- [23] Rubel, M., Brunsell, P., Duwe, R., Linke, J., Fusion Eng. Des. **49&50** (2000) 323.
- [24] Samm, U., et al., J. Nucl. Mater. **162–164** (1989) 24.
- [25] Goforth, R.R., et al., Nucl. Fusion **26** (1986) 515.
- [26] Denner, T., Finken, K.H., Mank, G., Noda, N., Nucl. Fusion **39** (1999) 83.
- [27] Taylor, J.B., Phys. Rev. Lett. **33** (1974) 139.
- [28] Zanca, P., Martini, S., Plasma Phys. Control. Fusion **41** (1999) 1251.
- [29] Wu, Chung Hsiu, Mszanowski, U., Martin, J.M.L., J. Nucl. Mater. **258–263** (1998) 782.
- [30] Linke, J., et al., Fusion Eng. Des. **49&50** (2000) 235.
- [31] Hedqvist, A., Rachlew-Källne, E., Plasma Phys. Control. Fusion **40** (1998) 1597.
- [32] Vietzke, E., Haasz, A.A., in Physical Processes of the Interaction of Fusion Plasmas with Solids (Hofer, W.O., Roth, J., Eds), Academic Press, New York (1996) Ch. 4, p. 135.
- [33] von Seggern, J., et al., Phys. Scr. T **81** (1999) 31.
- [34] Wienhold, P., et al., Phys. Scr. T **81** (1999) 19.
- [35] Rubel, M., Wienhold, P., Hildebrandt, D., J. Nucl. Mater. **290–293** (2001) 473.
- [36] Esser, H.G., et al., J. Nucl. Mater. **266–269** (1999) 240.
- [37] Koch, R., et al., “Low loop voltage start-up of the TEXTOR-94 discharge with ICRF and/or NBI assistance”, in Controlled Fusion and Plasma Physics (Proc. 26th Eur. Conf. 1999), Vol. 23J, European Physical Society, Geneva (1999) 745.
- [38] Lyssoivan, A., et al., *ibid.*, Vol. 23J, p. 737.
- [39] Kálvin, S., Mank, G., “Simulation of carbon pellet ablation and pellet expansion in a magnetized high temperature plasma”, in Carbon Materials (Proc. 9th Int. Workshop, Hohenkammer, 2000), [http://www.kfa-juelich.de/ipp/publication/veroeffentlichungen\\_2000.pdf](http://www.kfa-juelich.de/ipp/publication/veroeffentlichungen_2000.pdf).
- [40] Linke, J., et al., Phys. Scr. T **91** (2001) 36.
- [41] Larsson, D., et al., Vacuum **48** (1997) 693.
- [42] Winter, J., et al., J. Nucl. Mater. **162–164** (1989) 713.
- [43] Samm, U., et al., J. Nucl. Mater. **222–224** (1995) 25.
- [44] Noda, N., Philipps, V., Neu, R., J. Nucl. Mater. **241–243** (1997) 227.
- [45] Philipps, V., et al., J. Nucl. Mater. **258–263** (1998).

- [46] Rubel, M., et al., J. Nucl. Mater. **283–287** (2000) 1089.
- [47] Philipps, V., et al., Plasma Phys. Control. Fusion **42** (2000) B293.
- [48] Pestchanyi, S., Würz, H., Phys. Scr. T **91** (2001) 84.
- [49] Federici, G., et al., Plasma–material interactions in current tokamaks and their implications for next-step fusion reactors, Nucl. Fusion (in press).

(Manuscript received 12 May 2000

Final manuscript accepted 29 March 2001)

E-mail address of M. Rubel: rubel@fusion.kth.se

Subject classification: I1, Te; I1, Re; K0, Te; K0, Re; F2, Te; F2, Re